INL/CON-17-43078-Revision-0

The Role of Anisotropy on the Self-Organization of Gas Bubble Superlattice

J. Gan, Y. Zhang, C. Sun, Y. Gao, L. He, D. Sprouster, L. Ecker, Yipeng Gao

September 2017

The INL is a U.S. Department of Energy National Laboratory
operated by Battelle Energy Alliance

INL/CON-17-43078-Revision-0

The Role of Anisotropy on the Self-Organization of Gas Bubble Superlattice

J. Gan, Y. Zhang, C. Sun, Y. Gao, L. He, D. Sprouster, L. Ecker, Yipeng Gao

September 2017

Idaho National Laboratory
Idaho Falls, Idaho 83415

http://www.inl.gov

Prepared for the
U.S. Department of Energy

Under DOE Idaho Operations Office
Contract DE-AC07-05ID14517

The Role of Anisotropy on the Self-Organization of Gas Bubble Superlattice

J. Gan[1], Y. Zhang[1], C. Sun[1], C. Jiang[1], Y. Gao[1], L. He[1], D. Sprouster[2], L. Ecker[2]
[1]Idaho National Laboratory, [2]Brookhaven National Laboratory

Program Scope

Self-organization of nanoscale void/gas bubble superlattices has been widely observed in irradiation experiments however yet to be well understood. The recent discovery of incoherent face-centered-cubic (fcc) Xe bubble lattice in body-centered-cubic (bcc) UMo challenges the widely accepted coherency between superlattices and matrices. A complete mechanistic understanding of bubble lattice self-organization may have a large impact to materials science and nuclear energy advancement, and is the objective of this project. The knowledge obtained through a coherent integration of experimental and computational approach will advance the current understanding of self-organization mechanisms of nanostructures under irradiation. To realize this goal, two appealing self-organization mechanisms previously proposed in open literatures have been identified: anisotropic elastic interaction between voids and kinetic anisotropy such as one-dimensional (1D) self-interstitial atoms (SIA) diffusion. For the first year, the focus is on the effect 1D diffusion using bcc Mo and W, with the former being elastically anisotropic while the latter isotropic. Efforts have been made to investigate the fundamental interaction between inert gas and metal matrices, the mechanism for void/bubble superlattice formation and their stabilities under irradiation and annealing, and the experimental conditions for bubble superlattice formation and evolution, and to establish advanced characterization techniques for bubble superlattice.

Recent Progress

Helium gas bubble superlattice (GBS) has been successfully produced in pure Mo and W by using ion implantation. Systematical experiments have been performed to determine the optimized implantation conditions for the GBS formation. The injection of helium gas ions to ~ 10 at.% at temperature of 0.2 T_m (T_m: melting temperature) produces well-aligned gas bubbles in both Mo and W. It suggests that the role of elasticity on GBS formation is weaker than that of SIA diffusion. Figure 1 (left) shows the representative TEM micrographs of GBS in Mo and W, the inset of fast Fourier transform (FFT) suggests a clear evidence of the ordering of helium gas bubbles on {110} planes. The lattice parameter of He GBS, estimated using FFT, is ~ 4.8 nm in Mo and ~ 5.2 nm in W. The average size helium gas bubble is ~ 1.5 nm for both Mo and W. However, the gas bubble lattice parameter strongly depends on the implantation temperature and ion flux. It is known that Xe GBS in irradiated U-10Mo fuel has high thermal stability. In-situ thermal annealing experiment was conducted in transmission electron microscopy to study the thermal stability of He GBS in Mo. The result shows superior thermal stability of He GBS up to 850˚C ($0.39T_m$) as shown in Fig. 1 (center and right). The significance of this thermal stability is on its great potential for 3D patterning for advanced functional material as well as the design of the advanced nuclear fuels with inherent property for the development of thermally stable fission gas superlattice with high gas inventory capacity operating at high temperature.

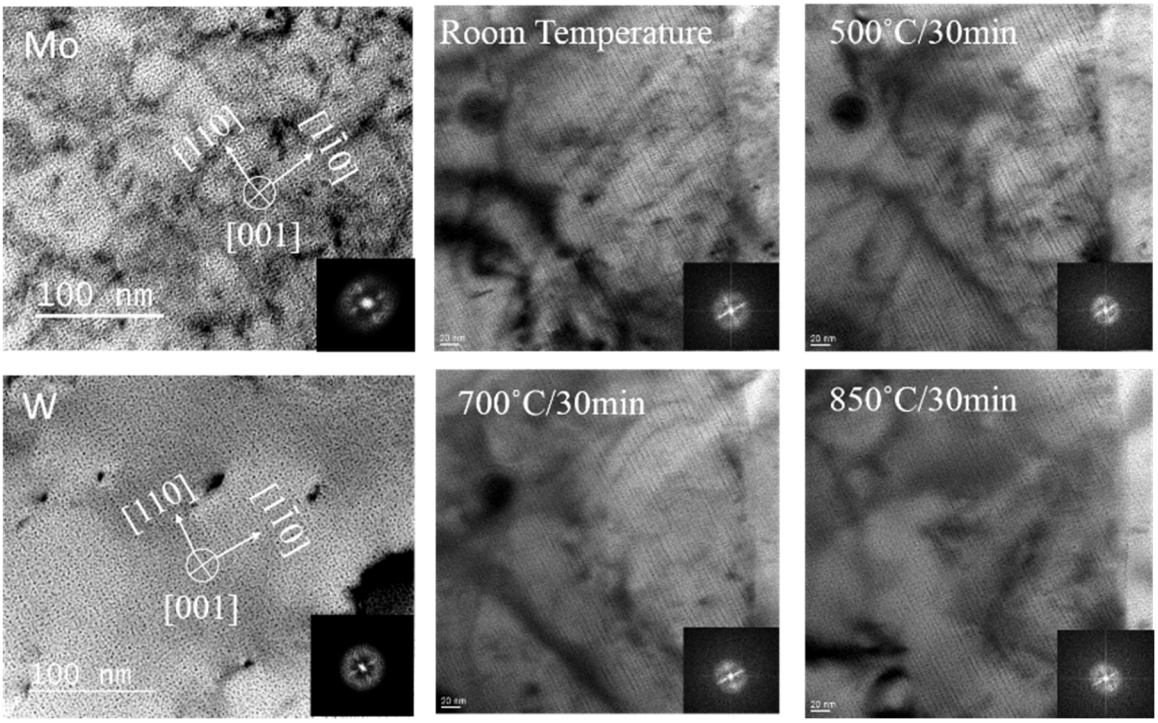

Figure 1. He gas bubble superlattice in Mo and W (left) using ion implantation. Insets with fast Fourier transform (FFT) show bubble ordering. TEM bright field images reveal stable He GBS alignment from in-situ annealing up to 850 ℃ (middle and right).

Irradiation-induced disordering of superlattice has been reported in the literature, for instance, ion irradiation can cause the disorder of L12 structured gamma prime precipitates in Ni-based suepralloy due to creation of point defects and anti-site defects. Here, the first time, the order-disorder transformation of He gas bubble superlattice is observed (Fig. 2) under Kr ion irradiation. TEM In-situ Kr ion irradiation with energy of 1 MeV using IVEM at ANL was performed on the Mo TEM foil with He GBS. The evolution of gas bubble alignment and FFT clearly suggests that the order-disorder transformation of He gas bubble superlattice under Kr ion irradiation at 300˚C completes at a relatively low dose of 2.5 dpa. This is quite different from Xe GBS in irradiated U(Mo) which is believed to be stable under irradiation.

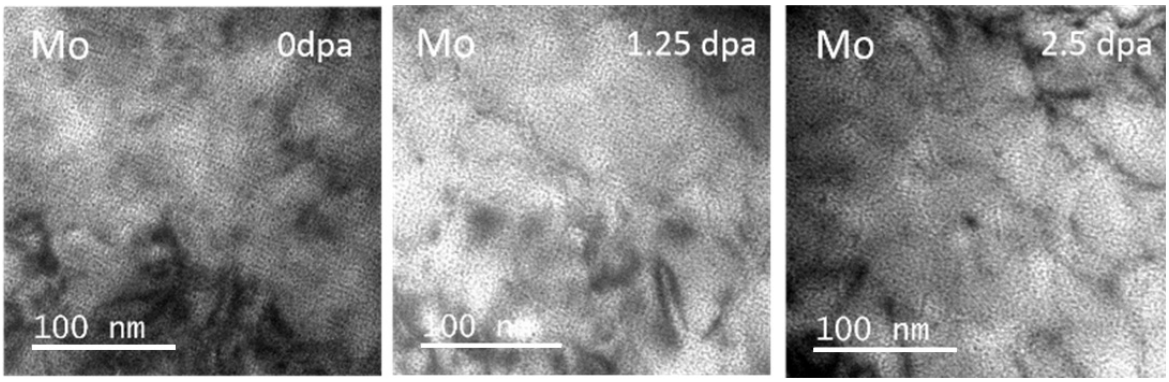

Figure 2. He gas bubble superlattice transformation from order to disorder under 1 MeV Kr irradiation at 300 ℃.

Systematical density functional theory (DFT) calculations have been carried out to explore the thermodynamic stability of inert gases such as He and Xe in group 5B (V, Nb and Ta) and 6B (Cr, Mo and W) metals, as well as the interactions between gas atoms and lattice defects. Some representative results are shown in Fig. 3. It is known that without vacancies the inert gases are found to have high solution energies in these metals. Accordingly, inert gas atoms show strong affinity to vacancies or voids, indicating a strong tendency to precipitate into bubbles. With sufficiently high gas to vacancy ratio in a gas-vacancy cluster, the presence of gas atom can effectively suppress recombination between vacancies and SIAs and stabilize this cluster, as shown by the increase in the interaction energy between a gas-vacancy cluster and a SIA in Fig.3. The results suggest high driving forces, particularly for Xe, to form stable gas bubbles under irradiation by occupying vacancies. These results provided thermodynamic basis for understanding gas behaviors in metal matrices and parameters to be used in atomistic simulations and theoretical analysis. Moreover, very good group trends are obtained in the results, suggesting that the interaction between inert gases and metal matrices may be governed by the electronic configurations of metal atoms.

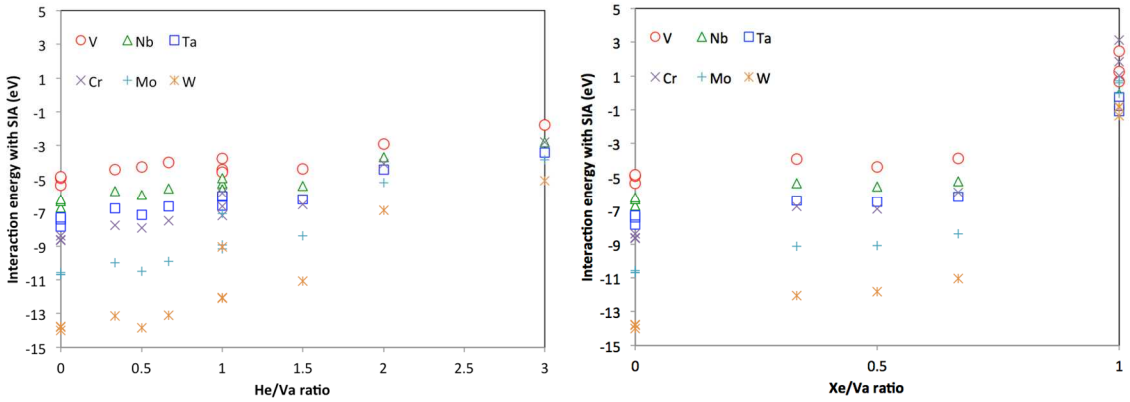

Figure 3. Interaction energies as a function of gas/vacancy ratio between a SIA and a gas-vacancy cluster in group V and VI bcc metals from DFT calculations.

To explore the nucleation process of void superlattice, which may possibly share the same formation mechanism with bubble superlattice, a novel atomic kinetic Monte Carlo (AKMC) method considering 1D SIA diffusion has been developed. In conjunction, theoretical analysis is carried out in analogy to phase separation in regular solution with source and reaction terms. It is predicted by the theoretical analysis that with increasing vacancy concentration, a critical condition will be reached for spontaneous phase separation, which features a characteristic length dependent on defect dynamics. This characteristic length can be stabilized when ordering is induced by kinetic anisotropy such as 1D SIA diffusion. The superlattice symmetry is found to be dictated by 1D SIA diffusion, challenging the widely accepted empirical rule that the superlattice is coherent with the matrix. The nature of spontaneous phase separation for superlattice is clear in AKMC simulations at low temperature and high dose rate, as shown in Fig. 4(a) and (c). With increasing temperature or decreasing dose rate, individual void nucleation and growth weaken the ordering, leading to *defects* formation in the superlattice, as shown in Fig. 4(b).

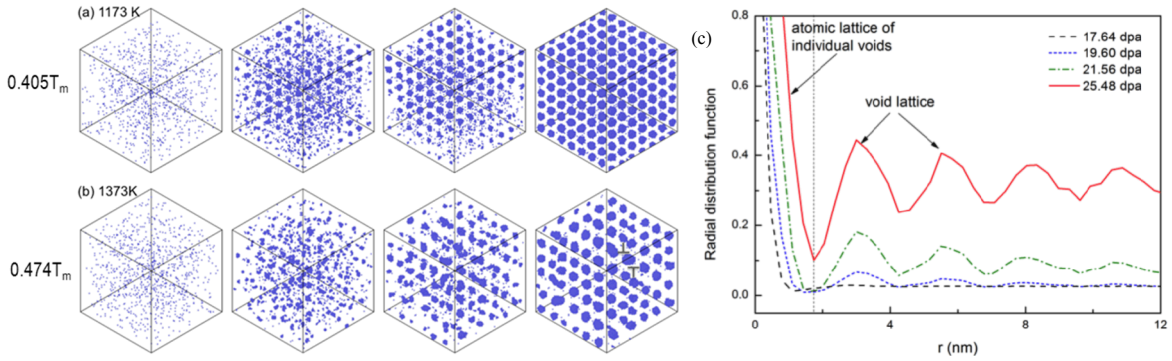

Figure 4. Snapshots of AKMC simulations showing 3D void lattice formation in Mo: (a) at 1173 K spontaneous phase separation leads to a perfect void lattice, and (b) at 1373 K, void nucleation and growth give defects in the void lattice. (c) Radial distribution function of vacancy showing the nucleation and stabilization of a wave length in the AKMC simulation shown in (a).

The theoretical analysis also leads to an analytical prediction of void superlattice parameter based on materials properties and irradiation conditions without any fitting parameters. The unprecedented predictability is demonstrated by comparison to independent experiments in W and Mo and AKMC simulations in Mo shown in Fig. 5. Three important trends regarding the superlattice parameter a_L are predicted: i) a_L increases with increasing temperature, ii) a_L decreases with increasing dose rate, iii) under the same irradiation condition, a_L is larger in materials with higher vacancy diffusivities. The first and the third predictions are validated by the measurements in neutron irradiated Mo and W in literature, and the second one is validated by AKMC simulations. An indirect experimental support to the second prediction is that, in general, at the same temperature the void superlattice parameters produced by ion irradiation are usually smaller than that by neutron irradiation, since the former is usually associated with much higher dose rates. Given the uncertainties in the experiments, quantitative comparison with experiments can be regarded as very good as well. The consistency between theory and experiments, alongside the direct support from AKMC simulations, indicates that the spontaneous phase separation based theory captures the nature of void superlattice formation. It can thus be utilized to tailor desired superlattice in experiments, e.g., by adjusting irradiation conditions and materials properties. This theory is expected to hold and will be extended for bubble superlattice.

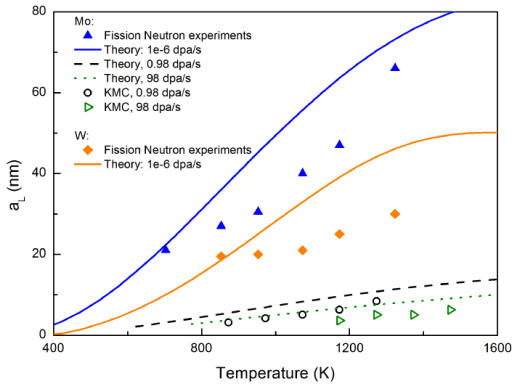

Figure 5. Superlattice parameters as functions of temperature in bcc Mo and W.

The above theoretical analysis also predicts a low temperature boundary for void superlattice formation using the condition that the predicted nearest neighbor distance in the superlattice is no less than twice of the recombination radius. In addition to void superlattice, the irradiation conditions for He gas bubble superlattice in bcc Mo and W have been identified experimentally. For both materials, bubble superlattices have been produced by He ion irradiation. Since both Mo and W have 1D SIA anisotropic diffusion and only Mo is elastically anisotropic, this confirms that indeed 1D SIA diffusion can lead to bubble superlattice formation, consistent with the AKMC simulations. Elastic anisotropy is not suggested as a necessary condition for that.

Synchrotron experiments at the NSLS-II at BNL were performed to nondestructively characterize bubble size, GBS lattice structure and lattice parameter in Mo and W substrates implanted with He ions. These were the first measurements of their kind and capitalized on the ultra-high brightness and small X-ray source size of the NSLS-II. Rapid SAXS and WAXS mapping measurements (< 20 min per sample) at the LiX beamline were performed to determine the spatial distribution of GBS within a series of samples.

An example of the SAXS-WAXS mapping is shown in Fig. 6(a) for a He implanted Mo sample. The mapping of SAXS and WAXS results in 1200 individual scattering/diffraction patterns. The visualization of GBS rich regions was accomplished with an image montage made possible through customized python scripts and ImageJ. The most intense scattering pattern in the center of the SAXS images (shown in red in Fig. 6(b)) is due to the signal from the matrix and He bubbles, while the diffuse diffraction spots observable away from the central pattern are attributed to the diffraction due to the ordering of the He gas bubbles.

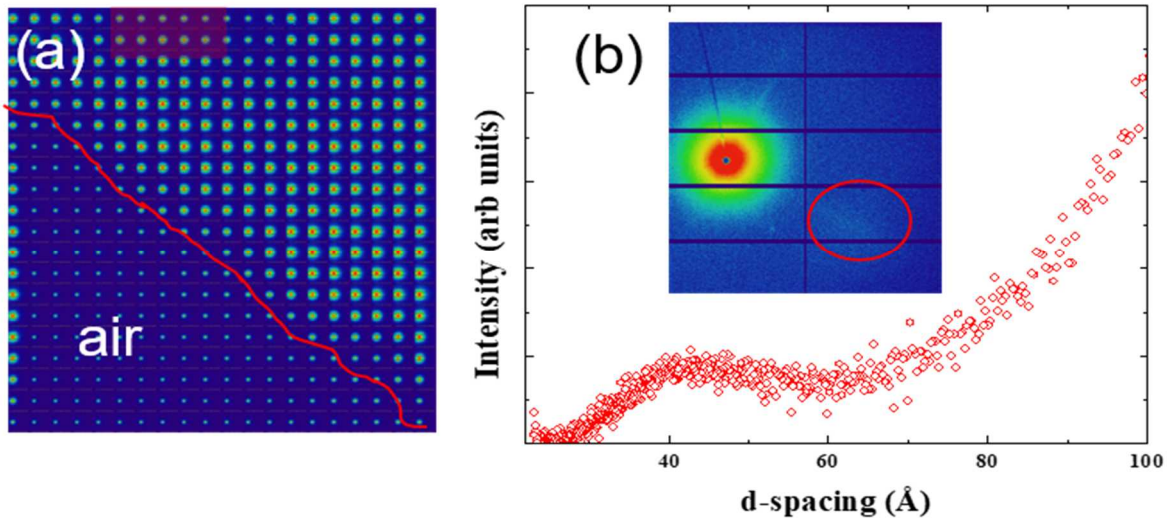

Figure 6. (a) SAXS map (montage of SAXS images) of a He implanted Mo sample. The sample surface is shown by a red line dividing a region with air scatter from the scattering from the sample. A portion of the GBS-rich region is highlighted (transparent red box). One of the integrated scattering patterns within the red box is shown in (b) with the diffraction peak from a plane of He GBS (d-spacing ~3.9 nm).

SAXS-WAXS experiments were also performed on a neutron irradiated U(Mo) nuclear fuel sample with well-developed Xe GBS at the LiX beamline (NSLS-II). Figure 7 shows an example of the scattering signal from the Xe GBS. The sharper, more well-defined diffraction signal is indicative that the fission gas bubbles are highly ordered, and phase identification shows that they are in an FCC arrangement, consistent with past TEM reports. Future synchrotron experiments on this sample include mapping the structural state of the gas in the GBS fine bubbles and in large fission gas bubbles that form in regions of the sample where the GBS has started to collapse with X-ray Absorption Near Edge Spectroscopy.

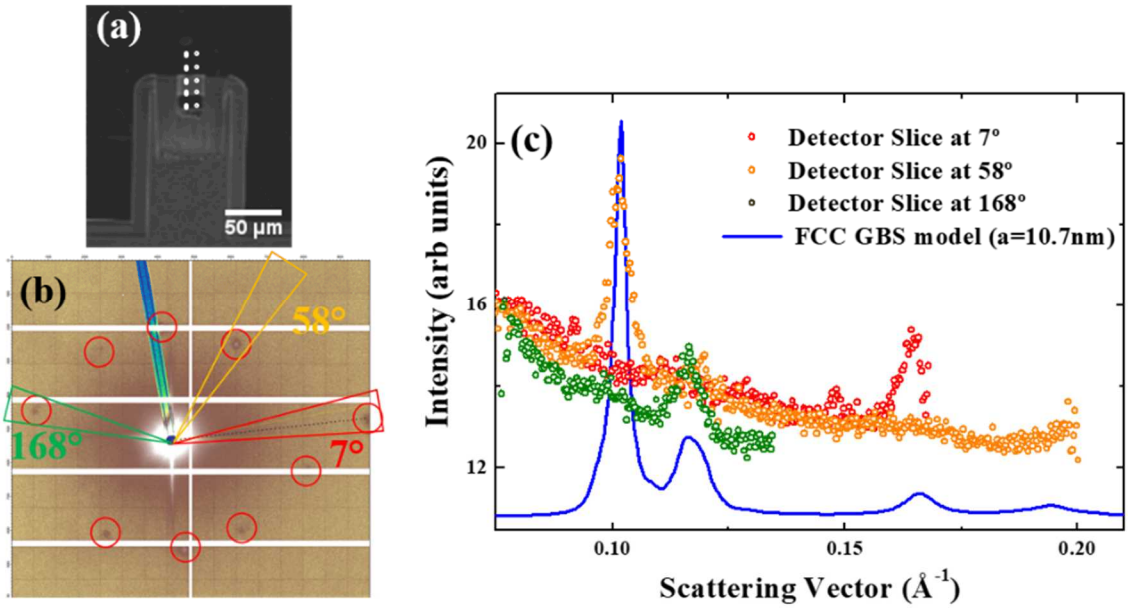

Figure 7. (a) Image of the neutron irradiated UMo fuel sample measured at LiX, (b) Scattering pattern with diffraction spots highlighted, (c) Intensity profiles of individual slices shown in (b) with the superposition of an FCC GBS model.

Future Plans

The accomplishments received so far have significantly advanced the current understanding on void/bubble superlattice formation. In the future, theoretical analysis will be continued to 1) predict superlattice symmetry based on anisotropic SIA diffusion, 2) predict bubble superlattice using the data produced by DFT calculations, and 3) to explore the role of elastic anisotropy. Trends regarding matrix properties, gas element, and irradiation conditions will be predicted. In conjunction, new experiments will be carried out to systematically study the effects of dose rate, temperature, matrix properties and gas elements on the gas bubble superlattice parameter, to validate the predictions by theoretical analysis. Advanced characterizations will also be done to quantify the strain field around the bubble and gas content and pressure in the bubbles.

References

1. J. Gan, D.D. Keiser, B. D. Miller, A. B. Robinson, D. M. Wachs, M. K. Meyer, Thermal stability of fission gas bubble superlattice in irradiated U-10Mo fuel, Journal of Nuclear Materials, 464 (2015): 1-5.
2. C. Sun, M. Kirk, M. Li, K. Hattar, Y. Wang, O. Anderoglu, J. Valdez, B. P. Uberuaga, R. Dickerson, S. A. Maloy, Microstructure, chemistry and mechanical properties of Ni-based superalloy Rene N4 under irradiation at room temperature, Acta Materialia, 95 (2015): 257-265.
3. C. Abromeit, S. Matsumura, Kinetics of antiphase domain boundaries during and L12 order-disorder phase transformation: a Monte Carlo simulation, Philosophy Magazine A, 82 (2002): 2287-2302.
4. J. H. Evans, Nature 29, 403 (1971).
5. N. M. Ghoniem, D. Walgraef, and S. J. Zinkle, Journal of Computer-Aided Materials Design 8, 1 (2001).
6. K. Malen and B. R., in Proc. Int. Conf. on Voids Formed by Irradiation of Reactor Materials, Reading (1971).
7. C. H. Woo and W. Frank, J. Nuclear Materials 137, 7 (1985).
8. J. W. Cahn, Acta Met. 9, 795 (1961).
9. J. Moteff, V. Sikka, and H. Jang, in Consultant Symp. on the physics of irradiation produced voids (1975).
10. J. DiFabio et al, "The Life Science X-ray Scattering Beamline at NSLS-II" AIP Conf. Proc. 1741, 030049 (2016)

Publications (Oct. 2016 – Aug. 2017)

Yipeng Gao, Yongfeng Zhang, Daniel Schwen, Chao Jiang, Cheng Sun, Jian Gan, Xian-Ming Bai, "Self-organization of void superlattices: atomic scale perspective and theoretical prediction", submitted to Nature Communication in August 14, 2017.

Four more journal articles are in preparation for submission in September 2017.